WARSAW UNIVERSITY OF TECHNOLOGY Index 351733
FACULTY OF CIVIL ENGINEERING
COMMITTEE FOR CIVIL AND WATER ENGINEERING
POLISH ACADEMY OF SCIENCES ISSN 1230-2945
DOI: 10.24425/ace.2026.158621
ARCHIVES OF CIVIL ENGINEERING
Vol. LXXII ISSUE 2 2026
pp. 467 –483

Research paper

Thermal-mechanical responses of steel portal frame under varying fire scenes with diverse protective measures

GuangPing Zhang[1], ZhaoBo Zhang[2], HongYuan Ma[3], HaiYang Liu[4], ChangHong Dong[5]

Abstract: This study investigates the thermal-mechanical responses of steel portal frame without fire pro-tection and with different fire protection strategies across three fire scenes. Temperature fields and heating curves were derived for the steel portal frame in three fire scenes using FDS simulations. Abaqus was employed to perform thermal-mechanical coupling simulations on the steel portal frame under eight conditions, both unprotected and protected with two types of fire protection. A comprehensive comparison and analysis of the simulation results yielded the following key conclusions: in all three fire scenes, the absence of fire protection and the implementation of two different fire protection measures lead to distinct failure modes in the steel portal frame, yet the lateral displacement response patterns remain consistent. Although fire protection strategies can delay the onset of displacement responses in the steel portal frame during fires, their effectiveness in reducing these responses is limited. Furthermore, fire-resistant boards alter the heat transfer path within the steel portal frame, increasing the temperature differential across the component sections and subsequently amplifying bending deformation. The findings provide valuable in-sights that enhance fire safety design for steel portal frame under diverse conditions.

Keywords: fire protection, fire scene, steel portal frame, thermal-mechanical response

[1]Eng., China Energy Engineering Group Gansu Electric Power Design Institute Co., Ltd., Lanzhou 730050, China, e-mail: zhangguangping8570@163.com, ORCID: 0009-0007-6669-610X
[2]PhD., College of Civil Engineering and Mechanics, Lanzhou University, Lanzhou 730000, China, e-mail: 120220908361@lzu.edu.cn, ORCID: 0009-0005-3399-6312
[3]Eng., China Energy Engineering Group Gansu Electric Power Design Institute Co., Ltd., Lanzhou 730050, China, e-mail: 1940704685@qq.com, ORCID: 0009-0003-0697-0219
[4]Eng., China Railway Construction Heavy Industry Corporation Limited, Changsha 410199, China, e-mail: 2901986623@qq.com, ORCID: 0009-0007-1783-3630
[5]Eng., China Energy Engineering Group Gansu Electric Power Design Institute Co., Ltd., Lanzhou 730050, China, e-mail: 1940704685@qq.com, ORCID: 0009-0003-0546-7953

1. Introduction

Steel portal frames are among the most prevalent structural forms in long-span steel constructions, widely used across various industrial applications, including substations, warehouses, and manufacturing facilities. However, due to the demands for expansive spaces by factors such as equipment layout or production process, the internal fire separation in steel portal frame is minimal, and the redundancy of its structure is limited. Consequently, in the event of a fire, the associated risks escalate significantly. Thus, investigating the thermal-mechanical response of steel portal frame under fire conditions holds paramount importance.

Currently, there is an increasing emphasis on assessing the safety of structures exposed to fire. In the field of thermal-mechanical response of steel portal frame under fire, researchers predominantly focused on temperature field and mechanical behavior under fire [1–5]. The fire's temperature field critically shapes the heating pattern of the steel portal frame, serving as a crucial determinant of its thermal-mechanical response. Lou et al. [6] executed a full-scale fire test on a steel portal frame plant, uncovering significant deviations of the actual temperature rise curve of the steel portal frame under real fire conditions from the standard heating curve. EI- Heweity [7] investigated the stress responses of portal frames and characterized the collapse modes by examining the sequence of plastic hinge formation. Shakil et al. [8] investigated the displacement responses of steel frames by analyzing geometric dimensions, load ratios, as well as different fire scenes, such as heated members and temperature distribution.

Implementing effective fire protecting measures substantially enhances the performance of steel structures in fire scenes. The focus of research on fire protection for steel structures is the thermal performance of fire protection materials. Silva et al. [9] investigated the thermal properties of a commercial water-based intumescent coating (IC) through experimental tests on steel plates with varying section factors and IC thicknesses. Their findings provide valuable insights for calibrating IC thermal properties in both simplified and advanced numerical models. Similarly, Lucherini et al. [10] investigated the effects of different heating conditions of two intumescent coatings (solvent-based and water-based) using three experimental setups under various fire scenarios. Their study highlights significant limitations in current design procedures for intumescent coatings, as their performance is highly dependent on heating conditions and fire heating rates. Cirpici et al. [11] introduced a methodology for predicting the fire resistance and thermal conductivity of intumescent fire retardant coatings under diverse conditions (different fire scenes, cross-sectional shape coefficients, and coating thicknesses). Bilotta et al. [12] performed fire tests on steel components protected by fire retardant coatings, demonstrating the coatings' ability to shield structural components from damage or excessive deformation. Raham et al. [13] investigated the fire behavior of steel portal frames under various support conditions and fire protection strategies. They recommended applying rotational restraints and fire protection to the columns to prevent outward collapse during a fire.

In summary, while research into the temperature field distribution within steel portal frame is well-advanced, studies on the fire resistance of steel structures with fire protection are relatively narrow, focusing mainly on the fire resistance properties of the materials themselves. There is a noticeable gap in research concerning the thermal-mechanical response characteristics of steel

portal frame with fire protection across various fire scenes. This paper sets out by employing FDS software to model three distinct fire scenes, yielding corresponding temperature rise curves. Subsequently, using Abaqus software, the thermal-mechanical response characteristics of steel portal frame protected by two fireproofing methods across multiple heating curves were examined. This led to insights into the fire resistance limits, failure modes, and displacement response patterns of the steel portal frame. Lastly, a systematic comparison and analysis of the fire resistance limits, failure modes, and displacement response patterns of steel portal frame protected under different fire scenes and fireproofing measures were performed, offering invaluable references for fire resistance design and selection of fireproofing measures for steel portal frame.

2. Methods

2.1. Structure information and numerical model

The GIS room of a substation employs a single-layer, single-span steel portal frame design, spanning 15 meters with column spacing of 7.5 meters, comprising 23 frames, column height of 16.8 meters, and an overall structure height of 18.3 meters. The H-shaped steel columns are designated as H600 × 300 × 12 × 14, while the H-shaped steel beams are specified as H600 × 250 × 12 × 14. Prior to the numerical simulation, the load-bearing capacity and deformation of the steel portal frame under ambient temperature loads were verified, confirming compliance with [14].

FDS (Fire Dynamics Simulator) software was engaged for modeling the fire temperature field, leveraging its capacity as a fluid dynamics simulation tool. As substantiated by experimental validations [15, 16], FDS can precisely replicate fire scenes. The analysis of thermal-mechanical coupling in steel portal frame is conducted using Abaqus, A model focusing on the steel portal frame coplanar with the fire source is established, mirroring the geometrical proportions of beams and columns outlined in section 2.1. Characteristics such as specific heat, thermal expansion coefficient, thermal conductivity, etc. comply with the specifications outlined in [17]. The outer face of the flanges on H-beams and columns facing away from the fire is designated as the unexposed (back) surface, with all remaining surfaces considered fire-exposed. Convective heat transfer coefficients and radiation coefficients are ascertained following [18–20], specifying 9 W/(m^2·°C) for the back surface and 25 W/(m^2·°C) for fire-exposed surfaces, alongside a radiation coefficient of 0.8.

2.2. Fire scenes setting

The fire source is positioned at the plane of 12th frame, at locations including the right column's foot and the mid-span ground of the frame. Three fire scenes are outlined as depicted in Table 1. The fire's duration is established at 10800 s (3 hours). For the acquisition of temperature field data, temperature measurement points are installed on the frame lying within the same plane as the fire source. The arrangement of all measurement points is illustrated in Fig. 1(a), representative measurement points are selected for analysis, as shown in Fig. 1(b).

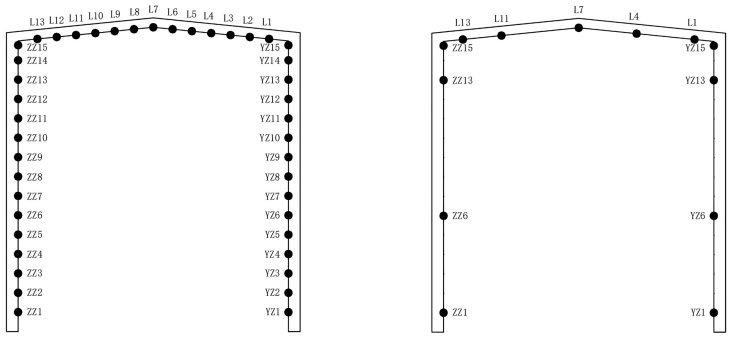

(a) (b)

Fig. 1. Measurement points layout: (a) All measurement Points, (b) Representative points

Table 1. Fire scenes

Fire scenes	Fire heat release rate (MW)	Fire source location
1	20	Right column foot
2	10	Right column foot
3	20	Mid-span ground

2.3. Criteria for Ultimate State Determination

The framework for defining the ultimate state of the steel portal frame encompasses three benchmarks: (1) holistic structural instability leading to failure; (2) deformations in components rendering them unfit for further loading; and (3) steel strains surpassing allowable limits. Regarding benchmark (2), This study imposes a vertical displacement limit for beams of 500 mm and a lateral displacement cap for a point on the column at 526 mm according to [21]. Concerning benchmark (3), adherence to posits that once the steel strain exceeds 0.2 under elevated temperatures, it signifies the attainment of the ultimate state [17].

3. Results analysis

3.1. Fire temperature field and temperature rise curves

3.1.1. Fire temperature field

Through simulation, the temperature field was obtained for three fire scenes. Due to space constraints, this section will exclusively discuss the temperature slice cloud of scene 1 at intervals of 500 s, 1000 s, and 2000 s, including horizontal temperature cloud at a height of 14.8 m, and temperature cloud perpendicular to the frame plane at mid-span, as depicted in Fig. 2 to Fig. 4. As evident from Fig. 2, the temperature field within the steel portal frame exhibits

pronounced stratification. The trajectory of the hot flue gas initiates at the foot of the columns, ascending to the column tops, whereupon it accumulates before flowing across the roof towards the top of the opposite column and descending. Fig. 3 reveals localized high temperatures at the column tops. These high-temperature zones expand over time, with the flue gas extending into the surrounding areas. It can be seen from Fig. 4 that the air temperature at mid-span perpendicular to the plane of the steel portal frame increases and stratifies significantly in the vertical direction, the air temperature continues to increase at higher elevations.

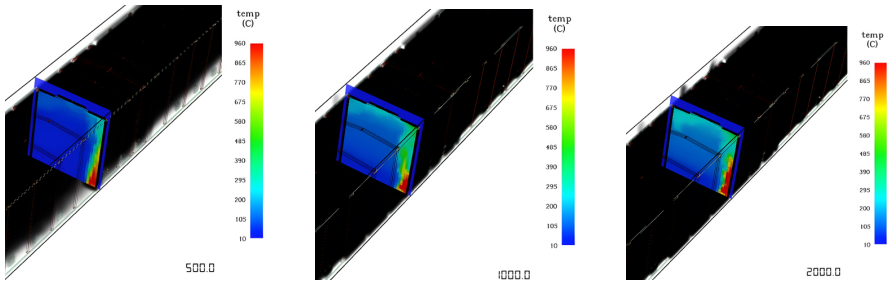

(a) (b) (c)

Fig. 2. Temperature slice cloud at the frame plane: (a) t = 500 s, (b) t = 1000 s, (c) t = 2000 s

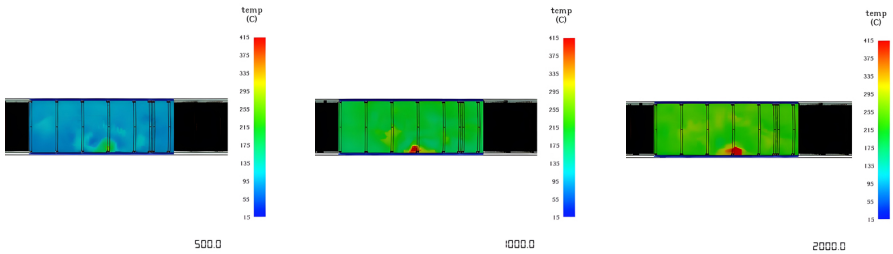

(a) (b) (c)

Fig. 3. Horizontal temperature slice cloud at the height of 14.8 m: (a) t = 500 s, (b) t = 1000 s, (c) t = 2000 s

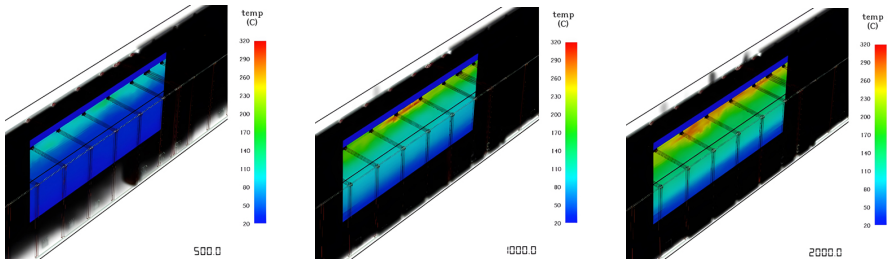

(a) (b) (c)

Fig. 4. Temperature slice cloud perpendicular to the frame plane at mid- span: (a) t = 500 s, (b) t = 1000 s, (c) t = 2000 s

The temperature-time curve for the designated measurement points on the frame is depicted in Fig. 5. Despite being farther from the fire origin and closer to the roof, sensor YZ15 records a higher temperature than sensor YZ13. This phenomenon results from the accumulation and subsequent heating of thermal smoke as it ascends from the ignition point to the roof. As demonstrated in Fig. 6, the interval from 0 to 1000 seconds (equivalent to 16 minutes) marks a phase of rapid temperature escalation at all measurement points. Between 1000 and 2000 seconds (or up to 33 minutes), the rate of temperature increase at each measurement points noticeably diminish. Beyond the 33 minutes mark, measurement points no longer register a consistent rise in temperature; instead, temperatures oscillate around a specific value.

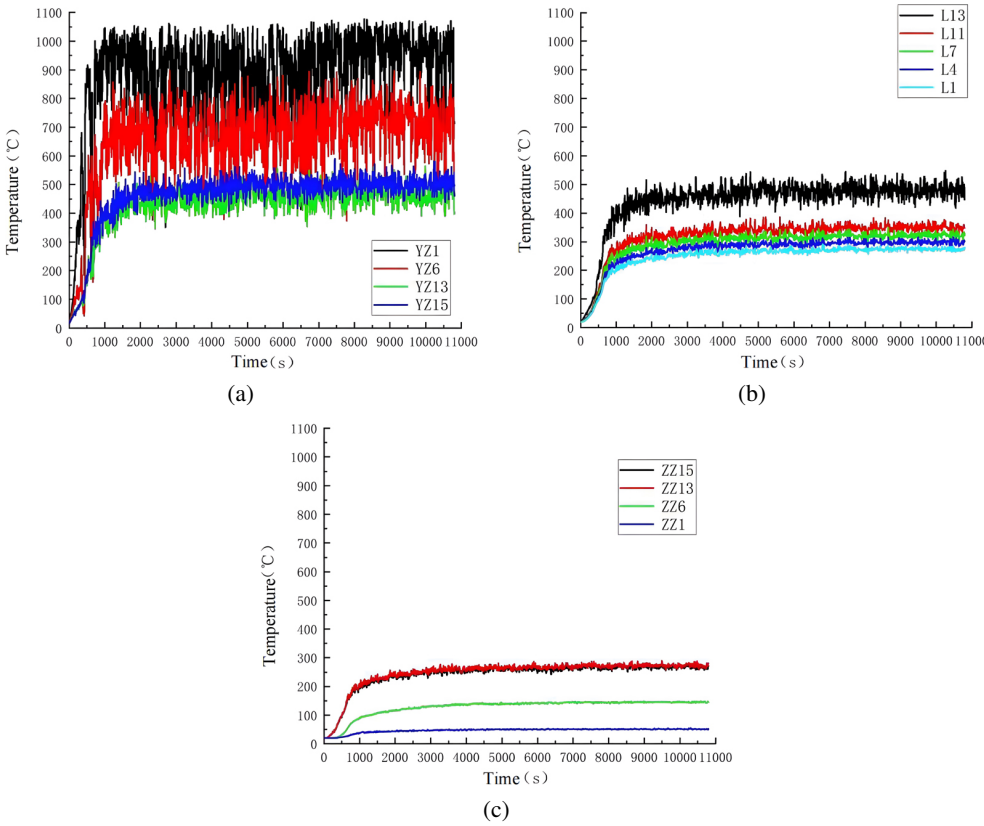

Fig. 5. Temperature-time curve of measuring points at beam and column: (a) Right Column, (b) Beam, (c) Left Column

Scene 2's temperature field is similar to scene 1, but with lower temperatures at all points. Conversely, scene 3 shows much lower temperatures near the frame, while the peak temperature is recorded at the midspan of the beam.

3.1.2. Temperature Rise Curves

The temperature-time curves derived from simulations reveal erratic fluctuations. Direct utilization of such data for analysis would not only substantially prolong the analytical process but also jeopardize the integrity of computational outcomes. Consequently, the necessity arises to refine these curves through fitting techniques. Averaging the original dataset for fitting purposes could underestimate safety margins, whereas employing envelope values proves overly cautious. This study adopts a fitting strategy wherein the temperature rise segment is modeled using a quadratic function. For fluctuating segments, the maximum average temperature value every 108 seconds from the raw data is adopted. A juxtaposition (Fig. 6) of the fitted heating curve for the right column foot with the standard heating curve reveals marked disparities between the two.

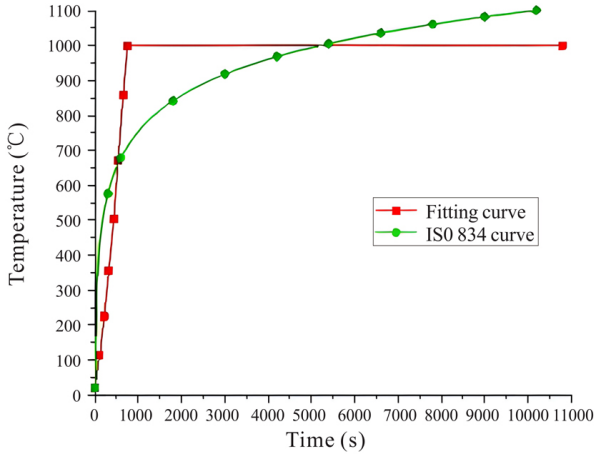

Fig. 6. Comparison of heating curves

3.2. Thermal-mechanical behavior of unprotected steel portal frame

The thermal-mechanical analysis initiating with computing the temperature distribution within the frame. Subsequently, this temperature field, coupled with ambient room temperature loads, is employed to perform a comprehensive thermal-mechanical interaction analysis over a duration of 3 hours (10,800 seconds). Temperature rise profiles are the same with the fitting curves of Section 3.2 along with a standard heating curve.

3.2.1. Fire scene 1

The horizontal displacement, vertical displacement, and equivalent plastic strain cloud (focusing on the column footing) at the steel portal frame's limit state are presented in Fig. 7. Observations from the figure indicate that at 1014 seconds (17 minutes) into the fire event, an area within the right column footing experiences an equivalent plastic strain surpassing 0.2, marking the attainment of the limit state. Prior to this critical point, both horizontal and vertical displacements of the steel portal frame remain minimal, significantly below their deformation thresholds.

A plot detailing the lateral displacement over time at the midpoint height of the right column (7.9 meters) is depicted in Fig. 8, where rightward movement denotes positive displacement. The analysis reveals an initial 15 mm rightward shift under ambient temperature loading conditions. Upon exposure to thermal loading, the column initially shifts further right, with the displacement rate escalating until it peaks at 42mm after 682 seconds (11 minutes). This is followed by a rapid leftward shift, reaching a maximum negative displacement of 35 mm at 907 seconds (15 minutes), and subsequently, the column swiftly moves right again until the right column footing hits its limit.

The initial rightward movement (0 to 682 seconds) is attributed to the greater thermal expansion on the fire-exposed side of the column due to a substantial temperature gradient early in the fire, causing the right column to bend rightward (depicted in Fig. 9(a)). The subsequent leftward motion (682 to 907 seconds) occurs as the stiffness of the right column reduces post-temperature increase, while the left column, generally cooler than its right counterpart during this interval, experiences more significant left- side thermal expansion due to local temperature differences, resulting in a leftward bend (Fig. 9(b)). Finally, the renewed rightward displacement (907 to 1014 seconds) is a consequence of the rapid rightward shift induced by the attainment of equivalent plastic strain in the high-temperature right column footing (Fig. 9(c)).

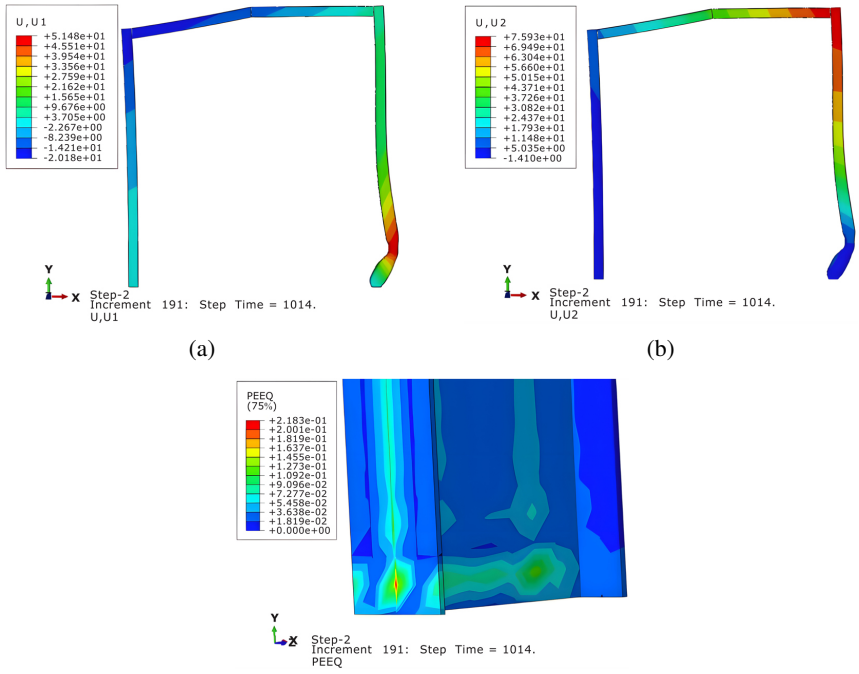

Fig. 7. Cloud of steel portal frame in limit state (scene 1): (a) Horizontal displacement cloud, (b) Vertical displacement cloud, (c) Equivalent plastic strain cloud

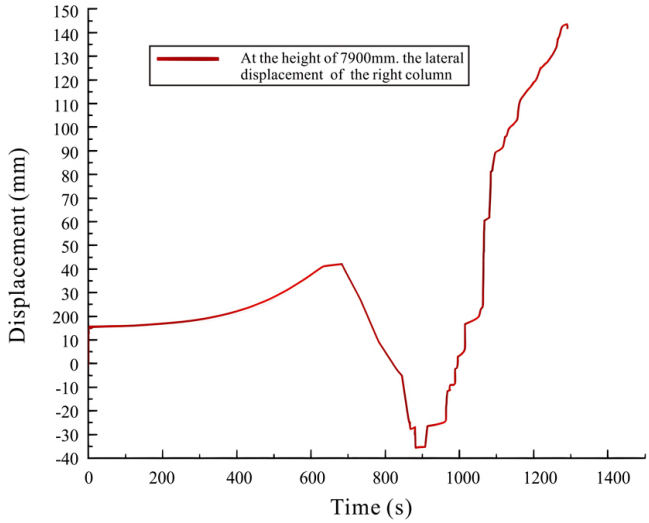

Fig. 8. The lateral displacement-time curve at half the height of right column (scene 1)

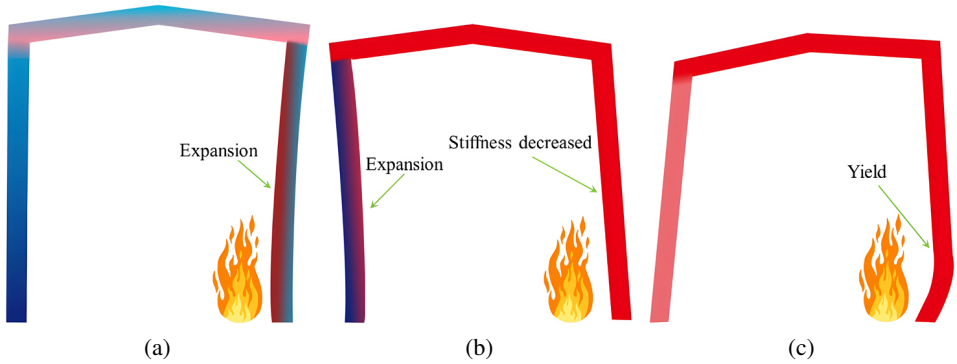

Fig. 9. Displacement changes of the steel portal frame (scene 1): (a) Shift to the right, (b) Shift to the left, (c) Shift to the right again

3.2.2. Fire scenes 2 and 3

Approximately 1426 seconds (24 minutes) into the fires, the right column footing sections in both scenes exhibit equivalent plastic strains surpassing 0.2, signifying the attainment of their respective limit states. Paralleling scene 1, prior to reaching these limit states, the horizontal displacements of the columns and the vertical displacements of the beams remain minimal, significantly beneath their deformation allowances. The pattern of horizontal displacement over time at the midpoint height of column in scene 2 mirrors that observed in scene 1. Moreover, scene 2's steel portal frame demonstrates a less pronounced displacement response and a prolonged fire resistance duration compared to scene 1. The steel portal frame in scene 3 does not reach its limit state even after 3.0 hours of fire exposure.

3.3. Thermal-mechanical response of the steel portal frame shielded by fire-retardant coatings

Sequential thermal-mechanical coupling analyses of the steel portal frame sharing the same plane with the fire source were conducted using Abaqus, with an analysis duration set at 3 hours. Two distinct fire-retardant coatings were selected and designated as the experimental group and control group, with their respective parameters sourced from [22]. The heating profiles utilized encompassed those from scene 1, scene 2, and the standard heating curve. The configuration of the working conditions is summarized in Table 2, EG stands for experimental group and CG stands for control group.

Table 2. Working conditions configuration of fire-retardant coating protection

Conditions	**1**	**2**	**3**	**4**
Type of coatings	EG	CG	CG	EG
Density (kg/m3)	637	400	637	637
Thermal conductivity (W·m–1·K–1)	0.191	0.1	0.191	0.191
Specific heat capacity (J·kg–1·K–1)	900	1100	900	900
Fire scenes	scene 1	scene 1	scene 2	ISO 834

3.3.1. Condition 1 and 2

Both condition 1 and condition 2 witness a shared failure mechanism: the steel portal frame's collapse is triggered when the equivalent plastic strain at the right column footing attains its limiting value, resembling the scene sans any fire protection. Differing thicknesses of fire-retardant coatings applied in conditions 1 and 2 lead to varied durations until the steel portal frame reaches its limit state, as summarized in Table 3. Evidently, the control group's fire-retardant coating demonstrates superior performance, effectively extending the timeframe until the steel portal frame hits its critical limit.

Table 3. Fire resistance limits (seconds) of condition 1 and 2

Thickness	**3 mm**	**5 mm**	**10 mm**
Condition 1	2591	5017	Limit state not reached
Condition 2	4135	6437	Limit state not reached

When fire-retardant coatings of varying thicknesses are applied, the lateral displacement time curves at the mid-height of the right column for scenes 1 and 2 are depicted in Fig. 10. All curves exhibit a congruent pattern of initial displacement to the right, followed by a shift to the left, and ultimately returning to the right, aligning with the lateral displacement behaviors and principles observed in unprotected steel portal frame within scene 1 and 2's thermal environments. As illustrated in Fig. 10, owing to scene 2's control group possessing superior fire-resistant properties, the lateral displacement curve at the mid-height of the right

column demonstrates a more gradual slope compared to scene 1. Furthermore, while the peak displacements in each segment are marginally reduced, this decrement is insignificant. In both scenes, an increase in the coating thickness leads to flatter displacement-time curves and diminished maximum displacements in respective segments. Consequently, applying a fire-retardant coating with enhanced fire-resistant capabilities and greater thickness can postpone the displacement response of steel portal frame exposed to fires, albeit with a negligible impact on reducing the magnitude of such responses.

3.3.2. Condition 1 and 3

Observations in condition 1 and 3 reveal an identical failure mechanism: the equivalent plastic strain at the foot of the right column reaching its threshold. Halving the fire's heat release rate fails to alter the failure mode of steel portal frame treated with fire-retardant coatings. Table 4 outlines the times taken for the steel portal frame, under condition 1 and 3 with varied coating thicknesses, to reach their failure states. The data illustrates that a 50% reduction in heat release rate elevates the fire resistance limit of the coated frames by over 40%. The temporal evolution of lateral displacement at the mid-height of the right column in condition 3 mirrors that of condition 1 (Fig. 10). In condition 3, applying the same fire-retardant coatings results in a smoother displacement curve compared to condition 1, but the extreme displacement values remain largely unchanged. This shows that reducing the fire's heat release rate slows displacement reactions but does not significantly reduce total displacement.

Table 4. Fire resistance limits (seconds) of conditions 1 and 3

Thickness	3 mm	5 mm	10 mm
Condition 1	2591	5017	Limit state not reached
Condition 3	3661	7071	Limit state not reached

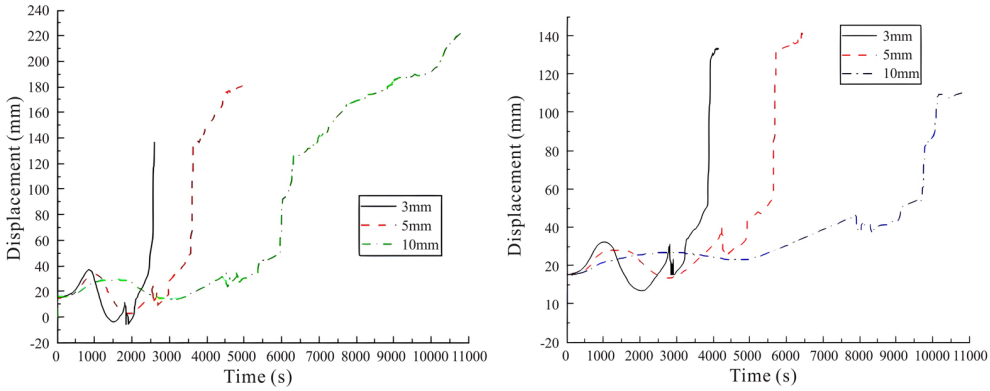

Figure continued on the next page

Figure continued from the previous page

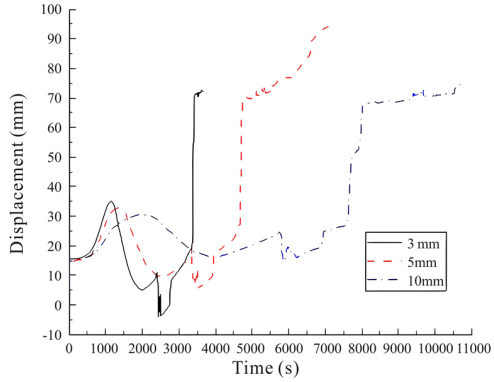

(c)

Fig. 10. The lateral displacement-time curve at the half height of right column: (a) Condition 1, (b) Condition 2, (c) Condition 3

3.3.3. Condition 1 and 4

Unlike condition 1, the failure mode of the steel portal frame in Condition 4 is characterized by the lateral displacement of the top of the right column exceeding the displacement limit of the ultimate state. When coated with a 10mm-thick fire-retardant coatings of the same type, the steel portal frame in condition 1 did not reach the ultimate state after 3 hours of fire exposure, while the steel portal frame in condition 4 reached the ultimate state at 4436 seconds (74 minutes) of fire exposure. Therefore, when a fire occurs at the column base, using the standard heating curve to analyze the thermal-mechanical response of the fireproof-coated portal frame results in a significant error.

3.4. Thermal-mechanical response of steel portal frame shielded by fire-resistant boards

Sequential thermal-mechanical coupling analyses were conducted on the steel portal frame coplanar with the fire source using Abaqus, with an analysis duration set at 3 hours. Gypsum board (GP) and calcium silicate board (CS) were selected as fire-resistant boards, with their respective thermal conductivities documented in Table 5 and Table 6. The density and specific heat capacity of GP and CS are referenced from [23]. The heating profiles considered comprised those of scene 1, scene 2, as well as the standard heating curve.

Table 7 outlines the working conditions: condition 5 and 6 examine the impact of fire-resistant board materials on the frame's thermal-mechanical behavior, condition 5 and 7 assess fire source intensity effects under consistent fire protection, and condition 5 and 8 explore the influence of fire scenes on the frame's resilience with fire-resistant boards.

Table 5. Thermal conductivity (λ) of GP

T (°C)	50	70	220	300	340	375	470	850	1000
λ	0.27	0.07	0.02	0.13	0.13	0.03	0.27	0.27	0.6

Table 6. Thermal conductivity (λ) of CS

T (°C)	35	80	250	360	385	420	880	920
λ	0.5	0.09	0.01	0.43	0.04	0.25	0.35	0.45

Table 7. Working conditions for fire-Resistant board protection

Working Conditions	5	6	7	8
Board material	GP	CS	GP	GP
Fire scene	scene 1	scene 1	scene 2	ISO 834

3.4.1. Condition 5 and 6

The collapse mechanism in condition 5 and 6 occurs when the steel at the right column foot reaches its ultimate plastic strain. Table 8 illustrates the instances at which condition 5 and 6 steel portal frame reach their limit states, revealing that the fire-resistant properties of both the gypsum board and calcium silicate board are essentially equivalent.

Table 8. Durations (seconds) of frames shielded by boards of diverse thicknesses

Working condition/thickness	**3 mm**	**5 mm**	**10 mm**
Condition 5	3778	5137	Limit state not reached
Condition 6	3753	5251	Limit state not reached

The lateral displacement-time curves at the mid-height of the right column for condition 5 and 6 are shown in Fig. 11. The curves exhibit a rightward shift, followed by leftward movement, and end with a final rightward drift, similar to patterns seen in unprotected or fire-coated steel portal frames. It is shown in Fig. 11 that applying fire-resistant boards makes the lateral displacement curve at the mid-height of the right column more gradual, thereby delaying the maximum displacement. However, condition 5 and 6 with 3 mm and 5 mm fire-resistant boards show higher first peak displacements compared to unprotected frames, while frames with 3 mm and 5 mm fire coatings exhibit lower peak displacements (refer to Fig. 10).

Inspection of the temperature distribution across the steel portal frame's cross-section reveals that under condition 5, at the moment of achieving the first rightward displacement extremity, the temperature differences between the midpoints of the inner and outer flanges at the half height of the right column stand at 118°C, 187°C, and 173°C for frames without

protection, with 3 mm boards, and 5 mm boards, respectively, with 3 mm yielding the highest discrepancy, followed by 5 mm, and no protection presenting the least. Under condition 6, similar displacement, the respective temperature gaps widen to 118°C, 211°C, and 218°C, positioning 5 mm as the most variant, 3 mm next, and no protection still the least. The heightened temperature differential across sections covered with fire-resistant boards is attributed to the altered heat transfer pathway. Specifically, the warming of the web and outer flange is significantly impacted by cavity radiation, which initially transfers heat less efficiently than conduction. This disparity in heat transfer efficiency exacerbates the temperature gradient across the component's cross-section, in turn amplifying the bending deformation of the structure.

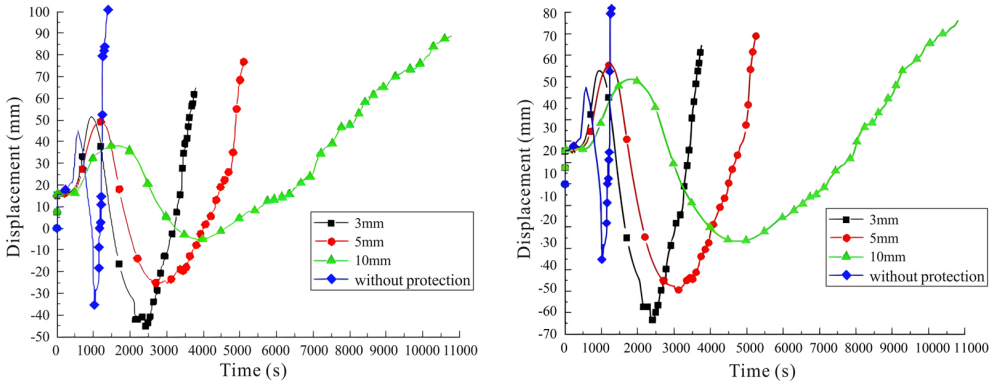

Fig. 11. Lateral displacement-time curve at the half height of right column: (a) Condition 5, (b) Condition 6

3.4.2. Condition 5 and 7

In contrast to condition 5, the steel portal frame in condition 7, clad with 3mm and 5 mm fire-resistant boards did not reach their limit state within 3 hours. Halving the fire's heat release rate significantly improved fire resistance. However, with fire-retardant coatings (condition 3), the equivalent plastic strain at the right column foot still reached its limit.

3.4.3. Condition 5 and 8

Diverging from condition 5, the failure mechanism in condition 8 involves the lateral displacement at the top of the right column surpassing the displacement limit for the limit state. The times at which steel portal frame under condition 5 and 8, clad with varying thicknesses of GP, reached their limit states are tabulated in Table 9. It is evident that the steel portal frame in condition 5, coated with a 10 mm-thick GP, did not reach its limit state after 3 hours of fire exposure, whereas its counterpart in condition 8, also with a 10 mm-thick GP, reached the limit state at 6029 seconds (1.6 hours), failing to fulfill the criterion of a fire resistance limit $\geq$ 2 hours. Hence, when a fire originates at the column foot, simulating the thermal-mechanical response of a fire-resistant board- protected steel portal frame using the standard heating curve introduces inaccuracies.

Table 9. Fire resistance limits (seconds) of condition 5 and 8

Thickness	**3 mm**	**5 mm**	**10 mm**
Condition 5	3778	5137	Limit state not reached
Condition 8	3502	4334	6029

4. Conclusions

This study investigates the thermal-mechanical responses of steel portal frame under varying fire scenes and different fire protection strategies. Using FDS and Abaqus simulations, the temperature field, failure modes, and displacement responses of steel portal frames with and without fire protection were analyzed, providing new insights into structural safety under fire Conditions. The primary findings are summarized as follows:

1. Temperature distribution characteristics

   In three distinct fire scenes, the temperature distribution within steel portal frame exhibits marked stratification, with their heating profiles diverging significantly from the standard heating curve. A reduction in the fire's heat release rate leads to an overall decrease in temperature without altering the spatial distribution of the thermal field.

2. Failure modes and fire endurance limits

   Lacking fire protection or with mere fire-retardant coatings, steel portal frame under the concurrent thermal and mechanical stresses of scenes 1 and 2 fail due to the equivalent plastic strain at the column foot nearest the fire exceeding its tolerable limit, causing failure. Conversely, frames fortified with fire boards in scene 1 succumb when the equivalent plastic strain at the foot of the column near fire source breaches its threshold.

   Employing standard heating curve for assessing the thermal-mechanical responses of frames with fire-retardant coatings or fire boards during fires initiating at column foot introduces conspicuous inaccuracies.

3. Displacement response law of the steel portal frame column

   Thicker fire-retardant coatings with better fire resistance can further delay the displacement response, although the reduction in displacement response is not significant. Lowering the heat release rate of the fire source can delay the displacement response of the frame during a fire, but it cannot reduce the displacement response.

   The heat transfer efficiency of cavity radiation is lower than that of heat conduction in the early stages of the fire, leading to a larger temperature gradient across the component section, which results in greater bending deformation of the component.

It is crucial to emphasize the need for further research. The statistical analysis approach can be employed to reconstruct the fire scene within the expansive space of the substation, based on the distribution of combustibles and their combustion characteristics. Future research may also explore the coating method that separates the fireproof board from steel members, while taking into account the thermal conductivity of the filler material.

References

[1] M. Rahman, et al., "Behavior of steel portal frames in fire: comparison of implicit and explicit dynamic finite element methods", *International Journal of Structural Stability and Dynamics*, vol. 13, no. 04, art. no. 1250058, 2013, doi: 10.1142/S0219455412500587.

[2] M. Maślak, M. Pazdanowski, M. Suchodoła, and P. Wozniczka, "Fire resistance evaluation for a steel hall transverse frame depending on the simplification degree of the computational model applied", *Archives of Civil Engineering*, vol. 68, no. 4, pp. 219–235, 2022, doi: 10.24425/ace.2022.143035.

[3] G.Q. Li, J. Han, G.B. Lou, and Y.C. Wang, "Predicting intumescent coating protected steel temperature in fire using constant thermal conductivity", *Thin-Walled Structures*, vol. 98, Part A, pp. 177–184, 2016, doi: 10.1016/j.tws.2015.03.008.

[4] A. Erfani and M. Dehestani, "Fire resistance behavior of damaged steel portal frame with RBS connections", *Journal of Constructional Steel Research*, vol. 182, art. no. 106698, 2021, doi: 10.1016/j.jcsr.2021.106698.

[5] P.A. Król, "Post-fire behavior and residual capacity of high- strength grade 8.8 steel bolts", *Archives of Civil Engineering*, vol. 70, no. 3, pp. 85–100, 2024, doi: 10.24425/ace.2024.150972.

[6] G. Lou, C. Wang, J. Jiang, Y. Jiang, L. Wang, and G. Li, "Fire tests on full-scale steel portal frames against progressive collapse", *Journal of Constructional Steel Research*, vol. 145, pp. 137–152, 2018, doi: 10.1016/j.jcsr.2018.02.024.

[7] M.M. El-Heweity, "Behavior of portal frames of steel hollow sections exposed to fire", *Alexandria Engineering Journal*, vol. 51, no. 2, pp. 95–107, 2012, doi: 10.1016/j.aej.2012.06.004.

[8] S. Shakil, W. Lu, and J. Puttonen, "Response of high-strength steel beam and single-storey frame in fire: Numerical simulation", *Journal of Constructional Steel Research*, vol. 148, pp. 551–561, 2018, doi: 10.1016/j.jcsr.2018.06.010.

[9] D. De Silva, A. Bilotta, and E. Nigro, "Experimental investigation on steel elements protected with intumescent coating", *Construction and Building Materials*, vol. 205, pp. 232–244, 2019, doi: 10.1016/j.conbuildmat.2019.01.223.

[10] A. Lucherini, L. Giuliani, and G. Jomaas, "Experimental study of the performance of intumescent coatings exposed to standard and non-standard fire conditions", *Fire Safety Journal*, vol. 95, pp. 42–50, 2018, doi: 10.1016/j.firesaf.2017.10.004.

[11] B.K. Cirpici, Y.C. Wang, and B. Rogers, "Assessment of the thermal conductivity of intumescent coatings in fire", *Fire Safety Journal*, vol. 81, pp. 74–84, 2016, doi: 10.1016/j.firesaf.2016.01.011.

[12] A. Bilotta, D. De Silva, and E. Nigro, "Tests on intumescent paints for fire protection of existing steel structures", *Construction and Building Materials*, vol. 121, pp. 410–422, 2016, doi: 10.1016/j.conbuildmat.2016.05.144.

[13] M. Rahman, J.B. Lim, Y. Xu, R. Hamilton, T. Comlekci, and D. Pritchard, "Effect of column base strength on steel portal frames in fire", *Proceedings of the Institution of Civil Engineers - Structures and Buildings*, vol. 166, no. 4, pp. 197–216, 2013, doi: 10.1680/stbu.11.00040.

[14] GB 51022-2015 Technical code for steel structure of light- weight building with gabled frames. Ministry of Housing and Urban-Rural Development of the PRC, 2015.

[15] S. Brohez and I. Caravita, "Fire induced pressure in airthigh houses: Experiments and FDS validation", *Fire Safety Journal*, vol. 114, art. no. 103008, 2020, doi: 10.1016/j.firesaf.2020.103008.

[16] J. Lee, B. Kim, S. Lee, and W.G. Shin, "Validation of the fire dynamics simulator (FDS) model for fire scenarios with two liquid pool fires in multiple compartments", *Fire Safety Journal*, vol. 141, art. no. 103892, 2023, doi: 10.1016/j.firesaf.2023.103892.

[17] EN 1993-1-2:2005 Eurocode 3: Design of steel structures - Part 1-2: General rules - Structural fire design. CEN, 2005.

[18] G. Thomas, "Modelling thermal performance of gypsum plasterboard-lined light timber frame walls using SAFIR and TASEF", *Fire and Materials*, vol. 34, no. 8, pp. 385–406, 2010, doi: 10.1002/fam.1026.

[19] M. Feng, Y.C. Wang, and J.M. Davies, "Thermal performance of cold-formed thin-walled steel panel systems in fire", *Fire Safety Journal*, vol. 38, no. 4, pp. 365–394, 2003, doi: 10.1016/S0379-7112(02)00090-5.

[20] P. Keerthan and M. Mahendran, "Numerical modelling of non- load-bearing light gauge cold-formed steel frame walls under fire conditions", *Journal of Fire Sciences*, vol. 30, no. 5, pp. 375–403, 2012, doi: 10.1177/0734904112440688.

[21] GB 50016-2014 Code for fire protection design of buildings. Ministry of Housing and Urban-Rural Development of the PRC, 2014.

[22] H. Wang, "Analysis of the fire resistance of steel structures exposed to temperature field based on FDS simulation", Harbin Institute of Technology, 2016.

[23] G. Fan, L. Wang, and W. Wang, "Experimental study on insulating properties of fire-resistant plates commonly used in building under different fire conditions", *Journal of Disaster Prevention and Mitigation Engineering*, vol. 42, no. 02, pp. 391–402, 2022, doi: 10.13409/j.cnki.jdpme.20210419001.

Received: 2025-01-17, Revised: 2025-02-11